On the Geometry of Isotropic Arrays

Ülkü Baysal, *Student Member, IEEE,* and Randolph L. Moses, *Senior Member, IEEE*

***Abstract*—We consider array geometries whose direction-of-arrival (DOA) estimation performance is isotropic. An isotropic array is one whose Cramér–Rao bound (CRB) on the DOA of a single source is uniform for all angles. For both planar arrays and volume arrays we derive necessary and sufficient conditions on array element locations so that the array is isotropic. We also present several designs of isotropic planar and volume arrays. The results apply to both narrowband and wideband scenarios.We analyze the special case where a planar array is used to estimate the DOA of three-dimensional (3-D) source. Finally, we compare isotropic array performance to the best possible array performance.**

***Index Terms*—Array geometry, DOA estimation, isotropic, wideband.**

I. Introduction

THE LOCATION of the elements in an array strongly affects the direction-of-arrival (DOA) estimation performance of the array. There has been a considerable amount of work done on the design of arrays to achieve or optimize desired performance goals that include terms such as cost, space, error variance, or resolution limits [1]–[6]. Much of the array design literature is devoted to linear arrays (or combination of linear arrays), perhaps because they are simple to analyze and because computationally efficient and effective DOA estimation algorithms are available for such arrays. On the other hand, linear arrays have nonuniform performance; the DOA estimation performance degrades considerably near endfire.

Several different performance and design criteria have been introduced to be used in obtaining optimal arrays. Performance comparisons of some common array geometries are presented in [7] and [8]. In [9], the authors introduce a measure of similarity between array response vectors and show that the similarity measure can be tightly bounded below. The array with the highest bound is optimum in the sense that it has the best ambiguity resolution. In [10], a sensor locator polynomial is introduced for array design. A polynomial is constructed using prespecified performance levels, such as detection-resolution thresholds and Cramér–Rao Bounds (CRBs) on error variance and its roots are the sensor locations of the desired linear or planar array. In [11], differential geometry is used to characterize the array manifold, and an array design framework based on these parameters is proposed.

Manuscript received April 26, 2002; revised November 27, 2002. This work was supported in part by the U.S. Army Research Office under Grant DAAH-96-C-0086. The associate editor coordinating the review of this paper and approving it for publication was Dr. Fulvio Gini.

The authors are with the Department of Electrical Engineering, The Ohio State University, Columbus, OH 43210-1272 USA.

Digital Object Identifier 10.1109/TSP.2003.811227

In this paper, we concentrate on arrays that have uniform performance over the whole field of view. We consider both planar and volume array geometries that have isotropic DOA estimation performance. For planar arrays, the arrays are isotropic in the sense that the CRB on the DOA estimation of a single source is uniform for all source arrival angles from 0 to 2π. For volume arrays, we use the bound on the mean square angular error (MSAE) as the criterion. The MSAE is a scalar measure of the error between true and estimated unit bearing vectors pointing toward the source, and its bound is computed from the CRB. The array is said to be isotropic if the bound on the MSAE is constant for all azimuth and elevation angles in $[0,\ 2\pi) \times (-(\pi/2),\ \pi/2)$. Since the CRB and bound on the MSAE are independent of any particular estimator and ML estimators asymptotically achieve these bounds, they are useful criteria for array design. Our results apply to both narrowband and wideband signals.

Arrays with uniform performance have been studied in various contexts. In his dissertation, MacDonald [12] considers isotropic arrays and presents conditions for isotropic performance. Hawkes and Nehorai [13] use the bound on the asymptotic mean square angular error to define an isotropic array. They derive the angle CRB for a single far-field source and give sufficient conditions on array geometry for the bound of the MSAE to be constant for all DOAs. Mirkin and Sibul [14] and Nielson [15] consider conditions on the array geometry for which the single source azimuth and elevation CRBs are uncoupled. Mirkin and Sibul [14] also derive a sufficient condition for isotropic planar array performance.

The present paper can be considered an extension and generalization of [12]–[15]. We provide necessary and sufficient conditions on isotropic array performance for both planar and volume arrays, thereby unifying and extending the results in [12]–[15]. In doing so, we summarize the results from [12], which are apparently not widely known in the array signal processing community. In addition, we develop a geometric interpretation of the isotropy condition that provides additional insight into the geometry of isotropic arrays and provides new methods for designing isotropic arrays. Finally, we provide simple bounds for comparing the performance of the optimal isotropic arrays to that of the optimal (anisotropic) array.

The organization of the paper is as follows. In Section II, we describe the system model and state our assumptions. Section III discusses the planar array scenario; we define the performance and isotropy conditions, give necessary and sufficient conditions on the array geometry for isotropic performance, and present several isotropic planar array design methods. In Section IV, we study the three-dimensional (3-D) arrays; we define the isotropy condition for this case, give necessary and sufficient conditions on the 3-D array for isotropic performance, and

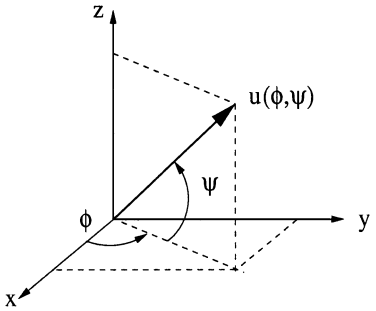

Fig. 1. Three-dimensional coordinate system showing the bearing vector $u(\phi, \psi)$ for a signal arriving from azimuth ϕ and elevation ψ.

provide some design methods. We also consider the isotropic performance when a planar array is used to estimate the DOA of a 3-D source. Section V presents a performance comparison between isotropic array and an array designed for optimal performance for a single source direction; we provide a bound on performance loss imposed by the isotropy condition for the geometry considered. Section VI concludes the paper.

II. System Model

We assume an array of N identical isotropic sensors located at r_i for $i \in [1, N]$. We will consider both planar arrays in which $r_i = [x_i, y_i]^T$ and volume arrays in which $r_i = [x_i, y_i, z_i]^T$.

Following [16], we adopt a system model describing a source impinging on the array. A single far-field source $s(t)$, which is, in general, wideband, impinges on the array from direction $\theta = [\phi, \psi]$, where ϕ denotes the azimuth angle measured counterclockwise from the x-axis on the x–y plane, and ψ denotes the elevation angle measured from the x–y plane (see Fig. 1). The noise at the sensors is assumed to be independent, zero mean, Gaussian, and independent of the source signal. The observation time T is partitioned into K intervals of length T_d and a J-point discrete Fourier transform is applied to each interval. Then [16]

$$x_k(\omega_j) = A_\theta(\omega_j)s_k(\omega_j) + n_k(\omega_j), \qquad \begin{matrix} j = 1, \ldots, J \\ k = 1, \ldots, K \end{matrix} \quad (1)$$

where $x_k(\omega_j)$, $n_k(\omega_j)$ are $N \times 1$ vectors, and $s_k(\omega_j)$ is a scalar. The elements of $x_k(\omega_j)$, $n_k(\omega_j)$, and $s_k(\omega_j)$ are the discrete Fourier coefficients of the sum of the sensor outputs, the noise, and the signal source at the discrete frequency ω_j, respectively. In addition

$$A_\theta(\omega_j) = \left[e^{j\omega_j d_1(\theta)}, e^{j\omega_j d_2(\theta)}, \ldots, e^{j\omega_j d_N(\theta)}\right]^T \quad (2)$$

where $d_k(\theta) = u^T(\theta) \cdot r_k/c$ is the propagation delay associated with the kth sensor, c is the speed of propagation, and $u(\theta)$ is the unit vector pointing toward the signal source (see Fig. 1). For a planar signal arriving from angle ϕ, $\theta = [\phi]$, and we denote $u(\theta)$ with $u(\phi)$; in this case

$$u(\phi) = [\cos(\phi), \sin(\phi)]^T. \quad (3)$$

For the 3-D case where a signal arrives from azimuth angle ϕ and elevation angle ψ, $u(\theta) = u(\phi, \psi)$, where

$$u(\phi, \psi) = [\cos(\phi)\cos(\psi), \sin(\phi)\cos(\psi), \sin(\psi)]^T. \quad (4)$$

Assuming T_d is long enough, the $x_k(\omega_j)$ vectors are uncorrelated.

III. Planar Arrays

In this section, we consider the special case of a planar array with elements on the (x, y) plane at locations $r_i = [x_i, y_i]^T$. The array is used to estimate the DOA of a wideband signal $s(t)$, which is coplanar with the array and arrives at an angle ϕ.

A. Single-Source CRB

For the system model described in Section II and under the planar array and coplanar signal assumptions, the CRB for the source DOA estimate is given by [16]

$$\mathrm{CRB}(\phi) = \frac{1}{2K}\left[\sum_{j=1}^{J}\frac{1}{n_j}\Re e\left\{\left(\dot{A}_\phi^H(\omega_j)P_{A_j}^{\perp}\dot{A}_\phi(\omega_j)\right) \odot \left(R_s(\omega_j) - \left(R_s^{-1}(\omega_j) + \frac{1}{n_j}A_\phi^H(\omega_j) \times A_\phi(\omega_j)\right)^{-1}\right)^T\right\}\right]^{-1}. \quad (5)$$

Here, $\dot{A}_\phi = dA/d\phi$ is the derivative of A with respect to the DOA angle ϕ, $P_A^{\perp} = I - A(A^HA)^{-1}A^H$ is the projection matrix onto the subspace orthogonal to the column space of A, $R_s(\omega_j) = E\{s_k(\omega_j)s_k^H(\omega_j)\}$ is the spatial covariance matrix of the impinging signals at frequency ω_j, and $\odot$ denotes the Hadamard product.

For the model given by (1) and (2), we find

$$\mathrm{CRB}(\phi) = [G(B, \phi) \cdot P]^{-1} \quad (6)$$

$$P = \frac{2KN}{c^2}\sum_{j=1}^{J}\frac{\omega_j^2}{n_j}p_j\left(1 - \frac{n_j}{p_jN + n_j}\right) \quad (7)$$

$$G(B, \phi) = \frac{du(\phi)}{d\phi}^T B \frac{du(\phi)}{d\phi} \quad (8)$$

$$B = \frac{1}{N}\sum_{i=1}^{N}(r_i - r_c)(r_i - r_c)^T \quad (9)$$

where r_c is the centroid of the array, i.e.,

$$r_c = \frac{1}{N}\sum_{i=1}^{N}r_i. \quad (10)$$

In (7), p_j is the signal power, and n_j is the noise power at frequency interval j.

We see that the CRB is a product of two terms. The first ($G(B, \phi)$) depends only on the source DOA ϕ and the array geometry through the matrix B; the second (P) depends on source

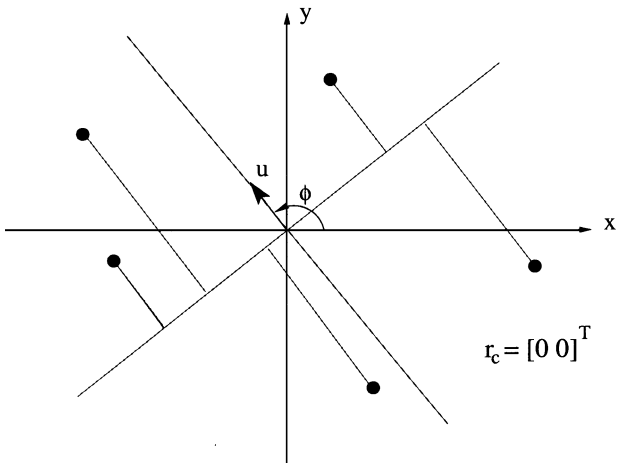

Fig. 2. Geometrical interpretation of $G(B,\ \phi)$ as the moment of inertia of the projected points of array locations onto the line orthogonal to $u(\phi)$.

and noise powers as a function of frequency. This is an important property because the impact of the array geometry on the CRB is the same, regardless of whether the source spectrum is narrowband or wideband, and regardless of the source signal and noise spectral densities. Thus, the results that follow apply to a broad class of array signal processing scenarios. Note that the matrix B is the 2×2 moment of inertia matrix of the array points. Any two array geometries that have the same moment of inertia matrices also have identical CRB performance.

We note that the array performance criterion we have chosen does not take into account potential array ambiguities that arise when the array manifold from two different DOAs are close to one another (see [9] for a discussion of this topic). Ambiguities are less of a problem for wideband arrays because the frequency diversity eliminates many DOA ambiguities [17].

B. Geometric Interpretation

We can write $G(B,\ \phi)$ explicitly in the following form:

$$G(B,\ \phi) = \sum_{i=1}^{N} (r_i - r_c)^T P_{u_\perp} (r_i - r_c) = \sum_{i=1}^{N} \|P_{u_\perp}(r_i - r_c)\|^2 \tag{11}$$

where $P_{u_\perp} = I - u(\phi)u^T(\phi)$ is a projection matrix. Equation (11) admits the following geometric interpretation [12]. Project the N sensor points onto a line orthogonal to the DOA ϕ and passing through the centroid; then, $G(B,\ \phi)$ is the moment of inertia of these projected points (see Fig. 2).

C. Beamwidth Interpretation

The parametric CRB measure of performance is also directly related to the nonparametric array beamwidth. To see this, consider an array that employs delay-and-sum weights, that is, the signals at each sensor are delayed to time-align signals arriving from angle ϕ_0, and then, these signals are summed to form the array output. Then, the complex-valued array response as a function of spatial angle ϕ and at frequency ω_0 and corresponding wavelength $\lambda_0 = 2\pi c/\omega_0$ is given by

$$W_{\phi_0}(\phi) = a^H(\phi)a(\phi_0) \tag{12}$$

$$a(\phi) = \left[e^{j(2\pi/\lambda_0)u(\phi)^T \cdot r_1},\ \ldots,\ e^{j(2\pi/\lambda_0)u^T(\phi)\cdot r_N}\right]^T. \tag{13}$$

A Taylor series approximation of the array gain $|W_{\phi_0}(\phi)|$ about the angle ϕ_0 yields (to second order)

$$|W_{\phi_0}(\phi)| \approx N - \frac{N}{2}\left(\frac{2\pi}{\lambda_0}\right)^2 G(B,\ \phi_0)(\phi - \phi_0)^2. \tag{14}$$

Using (14), the half-power beamwidth of the array is given by $(\lambda_0/2\pi)\sqrt{1/G(B,\ \phi_0)}$ and is thus linearly proportional to the square-root of the CRB for estimating ϕ_0 [see (6)]. Thus, the parametric CRB performance measure also has a nonparametric interpretation of array beamwidth.

D. Isotropic Planar Arrays

From (8), we see that $G(B,\ \phi)$, as well as the single-source CRB, is independent of translation of the array element locations; therefore, without loss of generality, we assume that the array is centered at the origin ($r_c = [0,\ 0]^T$). Under this assumption, B in (9) simplifies to

$$B = \frac{1}{N}\sum_{i=1}^{N} r_i r_i^T. \tag{15}$$

We are interested in planar array geometries whose single-source CRB is independent of signal arrival angle ϕ. We refer to such arrays as *isotropic arrays*. The following result gives necessary and sufficient conditions on the element locations of an array so that the array is isotropic.

Theorem 1: Let an N-element planar array have elements located at $r_i = [x_i,\ y_i]^T$ and be centered at the origin (that is, $\sum_{i=1}^{N} r_i = 0$). Then, the array is isotropic if and only if

$$B = kI_2 \tag{16}$$

where B is given by (15), I_2 is the 2×2 identity matrix, and k is a positive constant.

Proof: Since B is symmetric and non-negative definite, we can write

$$B = [e_1\ e_2]\begin{bmatrix}\lambda_1 & 0\\ 0 & \lambda_2\end{bmatrix}\begin{bmatrix}e_1^T\\ e_2^T\end{bmatrix} \tag{17}$$

where $\lambda_1 \geq \lambda_2 \geq 0$ and where λ_i is the eigenvalue corresponding to eigenvector e_i. Substituting (3) and (17) into (8) gives

$$G(B,\ \phi) = \lambda_1 \cos^2\beta + \lambda_2 \sin^2\beta \tag{18}$$

where β is the angle between $u(\phi)$ and e_2 ($\cos\beta = e_2^T u(\phi)$). We find from (18) that $G(B,\ \phi)$ is constant for all ϕ if and only if $\lambda_1 = \lambda_2$. ■

A geometric interpretation of Theorem 1 follows from (17); using the decomposition given in (17), B can be represented as an ellipse in $\mathcal{R}^2$ (see Fig. 3). If $\lambda_1 = \lambda_2$ (i.e., the array is planar

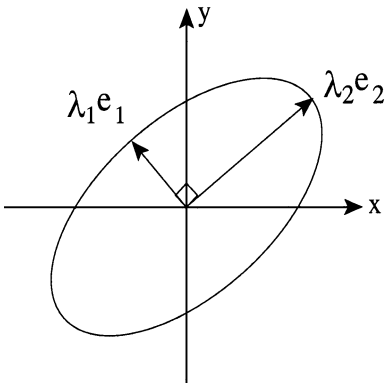

Fig. 3. Ellipse representation of the symmetric, nonnegative definite matrix B.

isotropic), the ellipse representation of B in Fig. 3 is a circle with radius λ_1.

Theorem 1 appears in [12]. The eigenvalue approach used in the proof appears to be new and leads to both a simpler proof and some new methods for designing isotropic arrays that are presented below.

Corollary 1: If an array is isotropic, then

$$G(B, \phi) = k = \frac{1}{2N} \sum_{i=1}^{N} \|r_i\|^2. \tag{19}$$

Proof: Substitution of (16) and (3) into (8) yields $G(B, \phi) = k$. In addition, with $B = kI_2$, (15) gives

$$\frac{1}{N} \sum_{i=1}^{N} x_i^2 = \frac{1}{N} \sum_{i=1}^{N} y_i^2 = k. \tag{20}$$

Thus

$$\frac{1}{N} \sum_{i=1}^{N} \|r_i\|^2 = \frac{1}{N} \sum_{i=1}^{N} \left(x_i^2 + y_i^2\right) = 2k \tag{21}$$

and (19) follows. ■

Finally, let $g = [g_1, \ldots, g_N]^T$, where $g_i = x_i + jy_i$ is the location of the ith sensor in the complex plane. Then, from the isomorphism between complex numbers and vectors, for an array centered at the origin ($\sum_{i=1}^{N} g_i = 0$), (16) holds if and only if

$$g^T g = 0 \tag{22}$$

meaning (22) is an equivalent necessary and sufficient condition for isotropy. The complex-plane formulation of array element locations is used in [14] and forms the basis of the isotropic design method in Section III-E4.

E. Isotropic Planar Array Design Examples

The constraint $B = kI_2$ leaves several degrees of freedom in which to design isotropic arrays; several design examples are presented below. The first two design methods are found in [12]; the remaining methods appear to be new.

1) Regular Polygon Designs: Define a *circularly symmetric* subarray as one in which $N \geq 3$ sensors are equally spaced on a circle with nonzero radius. A single sensor located at the origin is also in this class. Then, it follows that (15) and (16) are satisfied for any circularly symmetric subarray or any superposition of circularly symmetric subarrays. An example geometry, where a four- and a three-element subarray are combined to form a seven-element array, is given in Fig. 4. Notice that radii of the subarrays may be equal or unequal, and the orientation angles of the two subarrays are arbitrary.

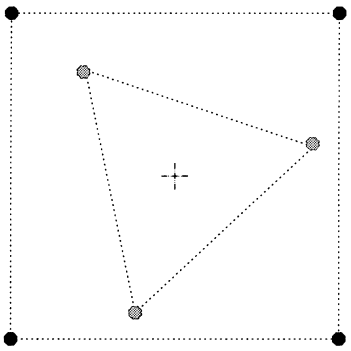

Fig. 4. Seven-element isotropic planar array obtained as the superposition of a four- and a three-element circularly symmetric array.

2) Isotropic Transformation: Given any N-element array centered at the origin whose array moment of inertia matrix is given by (17) with $\lambda_1 > \lambda_2$, then an isotropic array can be found by either "stretching" the array in the e_2 direction or by shrinking it in the e_1 direction. Specifically, if the sensor locations are transformed from

$$r_i = \alpha_i e_1 + \beta_i e_2 \tag{23}$$

to

$$\tilde{r}_i = k \left[\alpha_i e_1 + \sqrt{\frac{\lambda_1}{\lambda_2}}\, \beta_i e_2 \right] \tag{24}$$

for any constant k, then the transformed array is isotropic.

3) Rotated Geometries: We propose a design method where an array and rotated version of the array are superimposed. Consider an $N/2$ element subarray, where N is even, with arbitrary sensor locations. Let the origin be the centroid of these points, and define a second $N/2$-element subarray by rotating the first subarray by either 90° or -90°. Then, the N-element superposition of these two subarrays is an isotropic array.

An intuitive explanation of the rotated geometry design follows from the subarray ellipses. Let $r_s = [r_1, r_2 \cdots r_{N/2}] = [r_x, r_y]^T$, where r_x and r_y are $1 \times (N/2)$, represent the element locations for the first subarray, and let $r_\perp$ denote the element locations of the rotated subarray. Define $B_1 = (1/N) r_s r_s^T$ and $B_2 = (1/N) r_\perp r_\perp^T$. Then, the ellipses corresponding to B_1 and B_2 are orthogonal (see Fig. 5), and the concatenation results in the sum $B = B_1 + B_2 = kI$. Specifically, let $r_s = [r_x, r_y]^T$; then, the $+90^\circ$ rotated subarray element locations are $r_\perp = [-r_y, r_x]^T$ and

$$B = \frac{1}{N} [r \quad r_\perp] \begin{bmatrix} r^T \\ r_\perp^T \end{bmatrix} = \frac{1}{N} \begin{bmatrix} r_x & -r_y \\ r_y & r_x \end{bmatrix} \begin{bmatrix} r_x^T & r_y^T \\ -r_y^T & r_x^T \end{bmatrix}$$
$$= \frac{1}{N} \begin{bmatrix} r_x r_x^T + r_y r_y^T & r_x r_y^T - r_y r_x^T \\ r_y r_x^T - r_x r_y^T & r_y r_y^T + r_x r_x^T \end{bmatrix} = kI.$$

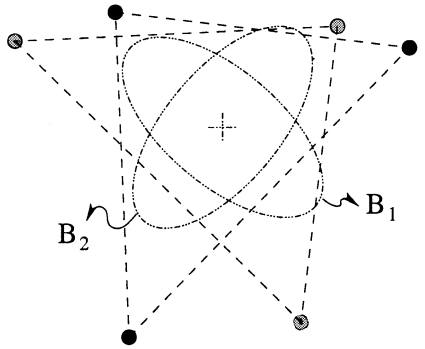

Fig. 5. Six-element isotropic array (black and gray points) formed from rotating a randomly generated three-element subarray (gray points) by 90°. Ellipses B_1 and B_2 corresponding to the original and rotated subarray, respectively, are also shown.

Hence, any geometry formed following this procedure is isotropic. For a -90° rotation, $r_\perp = [r_y, -r_x]^T$ and the proof follows similarly.

An example six-element array, generated by randomly selecting the locations of the first three elements, is shown in Fig. 5.

More generally, one can take any arbitrary subarray of size N/m and combine its $0, 2\pi/m, \ldots 2\pi(m-1)/m$ rotated versions about any arbitrary point (not just the center of gravity); the resulting N elements form an isotropic array. This array is also a superposition of m N/m-element circularly symmetric geometries, however, and is equivalent to the design in Section III-E1.

4) Completion of Arbitrary Arrays: We propose another design method where an N-element isotropic array is formed from an arbitrary $(N-2)$-element array by adding two elements. Assume that locations of the first $(N-2)$ sensors are given, and let r_{N-1} and r_N denote the locations of the remaining two sensors. Setting $\sum_{l=1}^{N} g_l = 0$ and $g^T g = 0$ [see (22)] gives

$$g_{N-1} + g_N = -\sum_{l=1}^{N-2} g_l \tag{25}$$

$$g_{N-1}^2 + g_N^2 = -\sum_{l=1}^{N-2} g_l^2. \tag{26}$$

The solutions to (25) and (26) uniquely determine the locations of the last two sensors such that the resulting N-element array is isotropic.

For the case that the centroid of the $(N-2)$ is the origin, the above solution has an intuitive geometric explanation. Let

$$\tilde{B} = \sum_{l=1}^{N-2} r_l r_l^T = [e_1 \quad e_2] \begin{bmatrix} \tilde{\lambda}_1 & 0 \\ 0 & \tilde{\lambda}_2 \end{bmatrix} \begin{bmatrix} e_1^T \\ e_2^T \end{bmatrix} \tag{27}$$

and assume $\tilde{\lambda}_1 \geq \tilde{\lambda}_2$. Then, it follows from (25) and (26) that

$$r_{N-1} = -r_N = \pm\sqrt{\frac{\tilde{\lambda}_1 - \tilde{\lambda}_2}{2}}\, e_2. \tag{28}$$

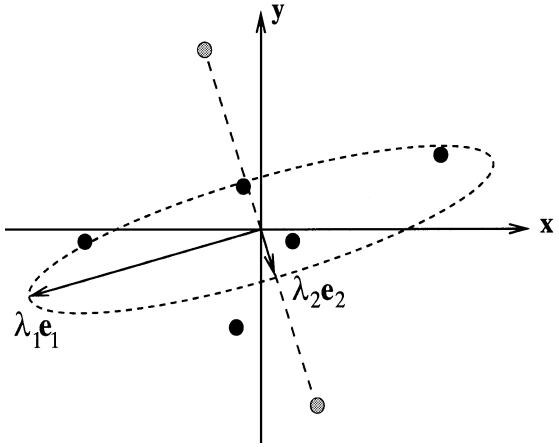

Fig. 6. Seven-element isotropic array formed from an arbitrary five-element subarray (black points) by adding two elements (gray points). The ellipse that represents $\tilde{B}$ in (27) is also shown.

Then, from (27) and (28), the moment of inertia matrix for the N-element array is

$$\begin{aligned} B &= \frac{1}{N}\sum_{l=1}^{N} r_l r_l^T \\ &= \frac{1}{N}\left(\tilde{\lambda}_1 e_1 e_1^T + \tilde{\lambda}_2 e_2 e_2^T + 2\,\frac{\tilde{\lambda}_1 - \tilde{\lambda}_2}{2}\, e_2 e_2^T\right) \\ &= \frac{\tilde{\lambda}_1}{N}\left(e_1 e_1^T + e_2 e_2^T\right) = kI. \end{aligned}$$

The last two array elements are placed along the minor axis of the ellipse corresponding to $\tilde{B}$ to make the moment of inertia in the e_2 direction equal to the moment of inertia in the e_1 direction, thus making $B = kI$. An example seven-element isotropic array formed from a randomly selected set of five elements is shown in Fig. 6.

5) X-Shaped Isotropic Arrays: We define an X-shaped geometry as a set of four sensors with distance d and angles $\pm\alpha, \pm(\pi - \alpha)$ from the origin. One can combine two or more properly-selected X-shaped geometries so that the resulting $4n$-element array (for $n = 2, 3, \ldots$) is isotropic. It is easy to verify that any pair of X-shaped geometries with parameters (d_i, α_i), $i = 1, 2$ that satisfy $d_1^2\cos(2\alpha_1) + d_2^2\cos(2\alpha_2) = 0$ is an isotropic array.

A special case is the superposition of X-shaped geometries are those whose elements lie along two lines. For two superimposed X-shaped geometries, we constrain $d_i \sin(\alpha_i) = c$ for all i. For example, an eight-element isotropic array with elements having y-values of ± 1 is shown in Fig. 7.

IV. Three-Dimensional Arrays

In this section, we consider an array that has elements located in R^3 and is used to estimate the DOA of a wideband far-field source. The source direction is parameterized by $\theta = [\phi, \psi]^T$, where $\phi \in [0, 2\pi)$ and $\psi \in (-(\pi/2), \pi/2)$ denote its azimuth and the elevation. The single source CRB for the direction of arrival is the 2×2 matrix

$$\text{CRB}(\theta) = [G(B, \theta)P]^{-1} \tag{29}$$

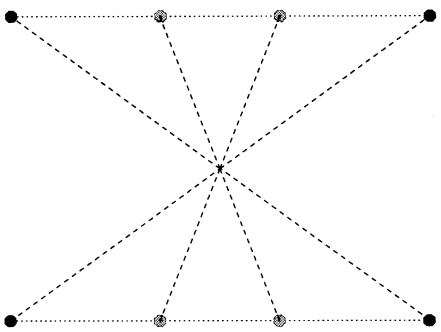

Fig. 7. Eight-element isotropic array formed by combining two X-shaped geometries.

$$G(B,\,\theta) = J_\theta(u)^T B J_\theta(u) \tag{30}$$

where $J_\theta(u)$ is the 3×2 Jacobian matrix of $u(\theta)$ in (4):

$$\begin{aligned} J_\theta(u) &= \left[\, \frac{\partial u(\theta)}{\partial \phi} \quad \frac{\partial u(\theta)}{\partial \psi} \,\right] \\ &= \begin{bmatrix} -\sin(\phi)\cos(\psi) & -\cos(\phi)\sin(\psi) \\ \cos(\phi)\cos(\psi) & -\sin(\phi)\sin(\psi) \\ 0 & \cos(\psi) \end{bmatrix} \end{aligned} \tag{31}$$

where B is given by (9), and where $r_i = [x_i,\, y_i,\, z_i]$ is the location of sensor i in $\mathcal{R}^3$. As in the planar case, the CRB is a product of two terms: The first ($G(B,\,\theta)$) depends only on the source DOA vector θ and the array geometry through the 3×3 matrix B; the second term depends on source and noise powers as a function of frequency.

A. Performance Criterion

Estimation of the source azimuth and elevation angles is equivalent to estimation of the vector $u(\theta)$: $\theta = [\phi,\, \psi]^T$ uniquely specifies $u(\theta)$ via (4), and an estimate $\hat{\theta} = [\hat{\phi},\, \hat{\psi}]$ uniquely specifies a similar vector $\hat{u}$. Let δ be the angle between the vectors u and $\hat{u}$; since both u and $\hat{u}$ are unit vectors, we have

$$\cos(\delta) = u^T \hat{u}. \tag{32}$$

The mean-square angular error (MSAE) is a scalar measure of estimator performance in estimating a geometrical vector and defined as the expectation of δ^2 [18]. The MSAE has two desirable properties: It is independent of the choice of the reference coordinate frame, and it does not suffer from the singularity inherent in spherical coordinates as $\psi \to \pm(\pi/2)$. The lower bound of the MSAE provides a performance criterion for a set of estimators that satisfies certain mild conditions that are similar to those needed for the CRB. A derivation for the lower bound of the MSAE and a detailed discussion of the conditions for the applicability and tightness of the bound can be found in [19]. Assuming K is the number of observations, the asymptotic normalized MSAE is defined as

$$\text{MSAE}_\infty = \lim_{K \to \infty} K E \delta^2. \tag{33}$$

The MSAE_∞ is bounded below by MSAE_B, which is given by

$$\text{MSAE}_\infty \geq \text{MSAE}_B = \cos^2(\psi)\text{CRB}(\phi) + \text{CRB}(\psi). \tag{34}$$

A geometric interpretation of MSAE_B is given in [13].

B. Isotropic Three-Dimensional Arrays

We adopt MSAE_B as a performance criterion and define a 3-D array to be isotropic if the associated MSAE_B is constant for all $[\phi,\, \psi]^T \in [0,\, 2\pi) \times (-(\pi/2),\, \pi/2)$. The following theorem defines the set of all isotropic 3-D arrays.

Theorem 2: Let an N-element volume array have elements located at $r_i = [x_i,\, y_i,\, z_i]^T$ and be centered at the origin (that is, $\sum_{i=1}^N r_i = 0$). Then, the array is isotropic if and only if

$$B = kI_3 \tag{35}$$

where B is given by (9), and k is a positive constant.

Proof: Consider the eigendecomposition

$$B = [e_1 \quad e_2 \quad e_3] \begin{bmatrix} \lambda_1 & 0 & 0 \\ 0 & \lambda_2 & 0 \\ 0 & 0 & \lambda_3 \end{bmatrix} \begin{bmatrix} e_1^T \\ e_2^T \\ e_3^T \end{bmatrix} \tag{36}$$

where e_1, e_2, and e_3 are orthonormal eigenvectors, and $\lambda_1 \geq \lambda_2 \geq \lambda_3 \geq 0$ are the corresponding eigenvalues. Note that $B = kI_3$ if and only if $\lambda_1 = \lambda_2 = \lambda_3 = k$.

Consider a source signal with $P = 1$ [cf. (7)], whose DOA is in the same direction as e_1, i.e., $\theta = \theta_1$, where $u(\theta_1) = e_1$. It follows from (30) and (31) that

$$G(B,\,\theta_1) = \begin{bmatrix} \lambda_2 \cos^2(\psi) & 0 \\ 0 & \lambda_3 \end{bmatrix} \tag{37}$$

$$\text{MSAE}_B(\theta_1) = \frac{1}{\lambda_2} + \frac{1}{\lambda_3}. \tag{38}$$

Similarly, if the same signal has DOA θ_2 such that $u(\theta_2) = e_2$, we find $\text{MSAE}_B(\theta_2) = 1/\lambda_1 + 1/\lambda_3$, and if its DOA is $=\theta_3$ such that $u(\theta_3) = e_3$, then $\text{MSAE}_B(\theta_3) = 1/\lambda_1 + 1/\lambda_2$. We see that $\text{MSAE}_B(\theta)$ is equal for $\theta \in \{\theta_1,\, \theta_2,\, \theta_3\}$ if and only if $\lambda_1 = \lambda_2 = \lambda_3$ or, equivalently, if and only if $B = kI_3$ with $k = \lambda_1$. ∎

Corollary 2: The function $G(B,\,\theta)$ corresponding to an isotropic volume array with $B = kI_3$ has the form

$$G(B,\,\theta) = k \begin{bmatrix} \cos^2\psi & 0 \\ 0 & 1 \end{bmatrix} \tag{39}$$

where

$$k = \frac{1}{3N} \sum_{i=1}^N \|r_i\|^2. \tag{40}$$

Proof: Substitution of $B = kI_3$ and (31) into (30) gives (39). In addition, inserting $B = kI_3$ in (15) yields

$$k = \frac{1}{N} \sum_{i=1}^N x_i^2 = \frac{1}{N} \sum_{i=1}^N y_i^2 = \frac{1}{N} \sum_{i=1}^N z_i^2. \tag{41}$$

Finally, using (41), we have

$$\frac{1}{N} \sum_{i=1}^N \|r_i\|^2 = \frac{1}{N} \sum_{i=1}^N \left(x_i^2 + y_i^2 + z_i^2\right) = 3k \tag{42}$$

from which (40) follows. ∎

We remark that isotropy is also a necessary and sufficient condition for the 2×2 CRB matrix to be of the form

$$\text{CRB}\left(\theta = \begin{bmatrix}\phi \\ \psi\end{bmatrix}\right) = \frac{1}{Pk}\begin{bmatrix}\dfrac{1}{\cos^2\psi} & 0 \\ 0 & 1\end{bmatrix}. \tag{43}$$

In this case, the CRB is diagonal, and the $1/\cos^2\psi$ term cancels the $\cos\psi$ compression of azimuth due to elevation angle ψ. Said another way, for an isotropic array, the CRB DOA uncertainty ellipse for a source, when mapped onto the unit sphere, is a circle whose radius is independent of the source DOA.

In [13], the authors give sufficient conditions on the array geometry so that MSAE_B is independent of the source signal DOA. Theorem 2 extends this result by proving that these conditions are also necessary. The theorem also extends results in [15] by establishing a link between isotropic arrays and array geometries for which $\text{CRB}(\theta)$ is diagonal.

C. Three-Dimensional Isotropic Array Designs

Analogously to the planar case, there are several ways to design isotropic volume arrays. Four such design methods are outlined below. The regular polyhedral design is mentioned in [12]; the remaining design methods appear to be new.

1) Polyhedral Designs: Arrays formed by placing the sensor elements at vertices of any regular polyhedron,[1] or a superposition of such arrays, result in three dimensional isotropic arrays. The result also holds for arrays whose elements are positioned at the vertices of the any of the 13 semiregular polyhedra. The result can be obtained by direct computation of (15) to establish that $B = kI_3$ for (semi)regular polyhedra centered at the origin and with vertices r_i.

2) Transformation-Based Designs: Similarly to the planar case, a given array with moment of inertia matrix B with eigendecomposition

$$B = \lambda_1 e_1 e_1^T + \lambda_2 e_2 e_2^T + \lambda_3 e_3 e_3^T \tag{44}$$

can be transformed to an isotropic array by stretching or shrinking the array in the unit directions defined by the eigenvectors.

3) Rotation-Based Designs: We propose a design to generate an N-element 3-D isotropic array from rotations of an arbitrary array of $N/3$ elements that are centered at the origin. Let

$$\begin{aligned}\tilde{B}_1 &= \frac{1}{N}\sum_{l=1}^{N/3} r_l r_l^T \\ &= \underbrace{\begin{bmatrix}e_1 & e_2 & e_3\end{bmatrix}}_{E}\begin{bmatrix}\tilde{\lambda}_1 & 0 & 0 \\ 0 & \tilde{\lambda}_2 & 0 \\ 0 & 0 & \tilde{\lambda}_3\end{bmatrix}\begin{bmatrix}e_1^T \\ e_2^T \\ e_3^T\end{bmatrix}.\end{aligned} \tag{45}$$

[1]There are five regular polyhedra: the tetrahedron, cube, octahedron, dodecahedron, and icosahedron.

The idea is to form two rotated $N/3$-element sets whose corresponding outer product matrices (similar to $\tilde{B}$ above) are, respectively

$$\tilde{B}_2 = E\begin{bmatrix}\tilde{\lambda}_2 & 0 & 0 \\ 0 & \tilde{\lambda}_3 & 0 \\ 0 & 0 & \tilde{\lambda}_1\end{bmatrix}E^T \tag{46}$$

and

$$\tilde{B}_3 = E\begin{bmatrix}\tilde{\lambda}_3 & 0 & 0 \\ 0 & \tilde{\lambda}_1 & 0 \\ 0 & 0 & \tilde{\lambda}_2\end{bmatrix}E^T. \tag{47}$$

Then, the N-element array has an outer product matrix given by

$$B = \tilde{B}_1 + \tilde{B}_2 + \tilde{B}_3 = (\tilde{\lambda}_1 + \tilde{\lambda}_2 + \tilde{\lambda}_3)I_3.$$

The rotated subarrays are found as follows: If $\tilde{r}_1 = [r_1, \ldots, r_{N/3}]$ are the elements of the given subarray and E is defined as in (45), then

$$\tilde{r}_2 = EJE^T\tilde{r}_1 \tag{48}$$

$$\tilde{r}_3 = EJ^TE^T\tilde{r}_1 \tag{49}$$

where

$$J = \begin{bmatrix}0 & 1 & 0 \\ 0 & 0 & 1 \\ 1 & 0 & 0\end{bmatrix}. \tag{50}$$

4) Completions of Arbitrary Arrays: We propose a design method in which three elements are added to an arbitrary $(N-3)$-element subarray to make the resulting N-element array isotropic. Let the $N-3$ element locations be given such that their centroid is at the origin. Define

$$\begin{aligned}\tilde{B} &= \sum_{l=1}^{N-3} r_l r_l^T \\ &= \begin{bmatrix}e_1 & e_2 & e_3\end{bmatrix}\begin{bmatrix}\lambda_1 & 0 & 0 \\ 0 & \lambda_2 & 0 \\ 0 & 0 & \lambda_3\end{bmatrix}\begin{bmatrix}e_1^T \\ e_2^T \\ e_3^T\end{bmatrix}\end{aligned} \tag{51}$$

where $\lambda_1 \geq \lambda_2 \geq \lambda_3 \geq 0$. Then, the three additional elements lie in the plane spanned by $\{e_2, e_3\}$. It is straightforward to verify that if

$$r_{N-2} = 2ae_3 \tag{52}$$

$$r_{N-1} = -ae_3 + \sqrt{b^2 - a^2}\,e_2 \tag{53}$$

$$r_N = -ae_3 - \sqrt{b^2 - a^2}\,e_2 \tag{54}$$

where

$$a = \tfrac{1}{2}\sqrt{\tfrac{2}{3}(\lambda_1 - \lambda_3)}, \qquad b = \sqrt{a^2 + \tfrac{1}{2}(\lambda_1 - \lambda_2)}$$

then the resulting N-element array is isotropic with $B = \frac{\lambda_1}{N}I_3$. If $\lambda_1 = \lambda_2 > \lambda_3$, then only two additional elements are needed at locations $\pm\sqrt{(\lambda_1 - \lambda_3)/2}\,e_3$.

D. Isotropic Planar Arrays for a 3-D Source

In this section, we consider the special case in which a planar array is used to estimate the elevation and azimuth of a 3-D source. The planar array is obtained by setting $z_i = 0$ for each element at location r_i, $i \in [1, N]$; thus, from (15), we have

$$B = \begin{bmatrix} B_{xy} & 0 \\ 0 & 0 \end{bmatrix} \tag{55}$$

where B_{xy} is a 2×2 matrix.

Mirkin and Sibul [14] derive conditions on a planar array geometry that ensures that the azimuth and elevation are uncoupled in the CRB. An uncoupled CRB is desirable because the azimuth estimation error is independent of whether or not the elevation of the source is known. They show that the CRB is uncoupled if and only if the array is (planar) isotropic. In this section, we establish that in this case, the CRB is also independent of azimuth, and it depends on elevation and array element locations in a simple way.

Theorem 3: Consider an N-element planar array centered at the origin and with elements located at $r_i = [x_i, y_i, 0]$ for $i = 1, \ldots, N$. Consider a source signal arriving from (spherical) direction $\theta = [\phi, \psi]^T$, where $|\psi| \in (0, \pi/2)$. Then, the CRB matrix for θ is diagonal and independent of azimuth ϕ if and only if

$$B_{xy} = kI_2 \tag{56}$$

for some positive constant k.

Proof: Let B in (55) have the eigendecomposition

$$B = [e_1 \quad e_2 \quad e_3] \begin{bmatrix} \lambda_1 & 0 & 0 \\ 0 & \lambda_2 & 0 \\ 0 & 0 & 0 \end{bmatrix} \begin{bmatrix} e_1^T \\ e_2^T \\ e_3^T \end{bmatrix} \tag{57}$$

where $\lambda_1 \geq \lambda_2 \geq 0$. Note that e_1 and e_2 can be written as

$$e_1 = [\cos\alpha, \sin\alpha, 0]^T, \quad e_2 = [-\sin\alpha, \cos\alpha, 0]^T \tag{58}$$

for some $\alpha \in [0, 2\pi)$. Then, from (30) and (31), we have

$$G(B, \theta) = \begin{bmatrix} G_{11} & G_{12} \\ G_{21} & G_{22} \end{bmatrix} \tag{59}$$

where

$$\begin{aligned} G_{11} &= \cos^2\psi \left[\lambda_1 \sin^2\beta + \lambda_2 \cos^2\beta\right] \\ G_{12} &= G_{21} = \sin\psi\cos\psi\left[\sin\beta\cos\beta(\lambda_2 - \lambda_1)\right] \\ G_{22} &= \sin^2\psi \left[\lambda_1 \cos^2\beta + \lambda_2 \sin^2\beta\right] \end{aligned}$$

and where $\beta = \alpha - \phi$. We thus see that for $\psi \in (-(\pi/2), \pi/2) - \{0\}$, $G(B, \theta)$ is diagonal and independent of ϕ if and only if $\lambda_1 = \lambda_2$. ■

Corollary 3: For a planar isotropic array as defined in Theorem 3, the CRB matrix of the source DOA is given by

$$\text{CRB}(\theta) = \frac{1}{Pk} \begin{bmatrix} \dfrac{1}{\cos^2(\psi)} & 0 \\ 0 & \dfrac{1}{\sin^2(\psi)} \end{bmatrix} \tag{60}$$

where ψ is the elevation angle of the source, and

$$k = \frac{1}{2N} \sum_{i=1}^{N} \|r_i\|^2. \tag{61}$$

Proof: Substitution of (55) and (56) into (29) and (30) gives (60). Equation (61) can be shown using the same argument as in Corollary 1. ■

We thus see from Theorem 3 and Corollary 3 that an isotropic planar array yields a CRB matrix in which the azimuth and elevation estimates are uncoupled, and conversely. Moreover, the CRB variances in the azimuth and elevation directions are independent of azimuth and depend on elevation in a simple geometric way.

V. Comparison of Optimal and Isotropic Geometries

In this section, we compare the performance of an isotropic array with that of an array optimized to have minimum DOA variance for a source at a single direction. We consider a simple case of an N-element planar array whose elements are constrained to lie on a disk of radius R. It can be shown that the array configuration that minimizes the CRB for a source arriving at an angle ϕ_0, which we call the ϕ_0-optimal array, is obtained by placing all elements at locations $Re^{j(\phi_0 \pm \pi/2)}$ [see Fig. 8(a)]. The corresponding value of $G(B, \phi)$ from (8) is NR for N even and $(N - (1/N))R$ for N odd. This array configuration is not a good practical choice because several elements are at identical locations; in practice, one would need to separate the array elements, say, by spreading them out along the disk boundary. While this array is optimal for sources at arriving at angle ϕ_0, its performance degrades as the DOA deviates from ϕ_0, as seen in Fig. 8(c).

The minimum variance isotropic array is found by placing the N sensors on the boundary of the disk, for example, by spacing them equally [see Fig. 8(b)]. Other spacings are possible depending on the value of N; see the first design method in Section III-E. We find from (19) that $G(B, \phi) = NR/2$. Thus, the isotropic array has DOA estimation variance that is twice the variance from the best array. Fig. 8(c) compares the CRB performances of the ϕ_0-optimal and the isotropic arrays.

A similar argument for volume arrays constrained to lie in a sphere shows that the MSAE_B of the isotropic array is a factor of 3 times the MSAE_B of the best array; this is a consequence of (35) and the factor 1/3 in (40).

VI. Conclusion

We have studied 2-D and 3-D arrays that have isotropic performance. For planar arrays, we have adopted the single source

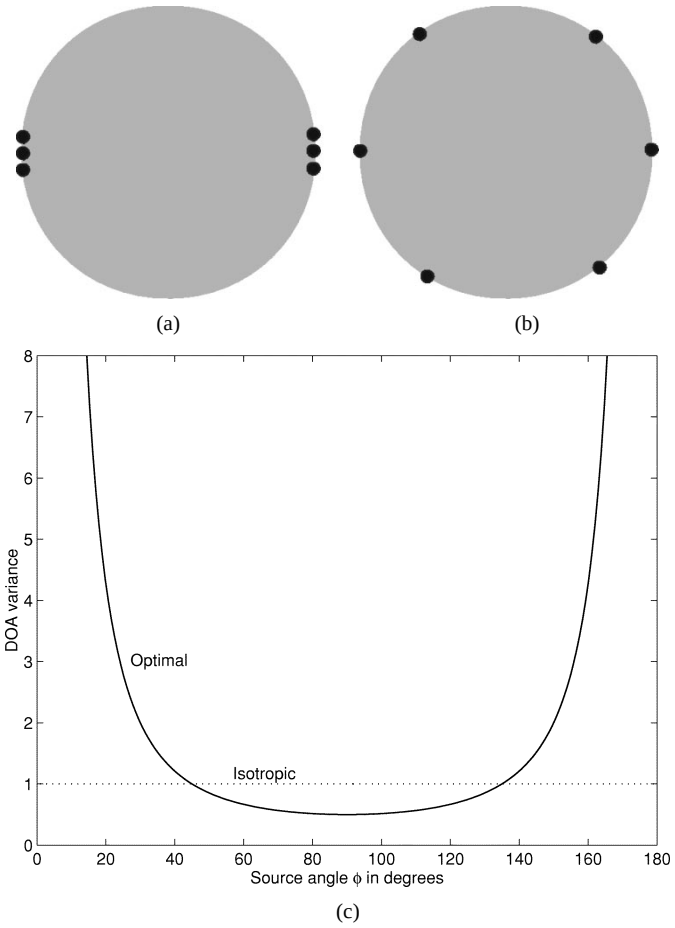

Fig. 8. Comparison of a ϕ_0-optimal array geometry and an isotropic array geometry when the elements of a planar array are constrained to lie on a disk. (a) ϕ_0-optimal array geometry for a source at $\phi_0 = \pm(\pi/2)$. (b) Isotropic array geometry. (c) Comparison of DOA estimation standard deviations for the two array geometries.

wideband Cramér–Rao bound as the performance criterion and have derived the necessary and sufficient conditions on the location of sensor elements so that the CRB of the source direction-of-arrival estimate is constant for all arrival angles. These conditions are valid regardless of the source's frequency spectrum. We also presented five methods to design isotropic planar arrays.

For 3-D arrays, we have used the bound on the asymptotic mean square angular error (MSAE_B) as a measure for array isotropy. We have derived necessary and sufficient conditions on the array geometry that ensure that the MSAE_B is independent of source azimuth and elevation arrival angle. When these conditions are satisfied, the azimuth and elevation are uncoupled in the CRB, and the CRB is independent of the source signal azimuth. We have also proven that when a planar array is used to estimate the DOA of a 3-D signal, the associated CRB is uncoupled in azimuth and elevation if and only if it is planar isotropic. An uncoupled CRB is desirable because the azimuth estimation error is independent of whether or not the elevation of the source is known [14].

Finally, a simple example comparing arrays optimized for a single source direction versus isotropic arrays showed that the isotropic planar array DOA variance is a factor of 2 times that of the best array (three times for a 3-D array). This suggests that isotropic arrays provide uniform performance at a modest decrease in performance as compared with arrays tuned for best performance at a single source direction.

The geometric interpretation of array isotropy provides insight into extension of practical interest. For example, in applications for which one is interested in array performance over a sector of DOAs, we see from the theorems that the conditions for isotropy remain unchanged as long as the sector has nonzero measure. In addition, arrays that are "almost isotropic" relate directly to the eigenvalue spread in the matrix B.

The isotropic arrays considered are derived under the assumptions of isotropic element gain and spatially isotropic noise power. These assumptions are reasonable for many acoustic or seismic array applications. Extensions to more general conditions, and extensions that incorporate practical array effects such as mutual coupling, would be of interest, especially in electromagnetic array applications.

When designing isotropic arrays, an important practical issue that should be taken into account is the minimum allowable distance between sensors. We have assumed the noise components at the sensors are independent of each other; this assumption is violated when the sensor distances become small (see [2]). Our design methods do not guarantee that the resulting sensors are sufficiently well-separated, so if the designs produce closely spaced sensors, they should be modified accordingly.

ACKNOWLEDGMENT

The authors wish to thank Dr. C. Burmaster for bringing [12] to our attention.

REFERENCES

[1] V. Murino, "Simulated annealing approach for the design of unequally spaced arrays," in *Proc. Int. Conf. Acoust., Speech, Signal Process.*, vol. 5, Detroit, MI, 1995, pp. 3627–3630.

[2] A. B. Gershman and J. F. Böhme, "A note on most favorable array geometries for DOA estimation and array interpolation," *IEEE Signal Processing Lett.*, vol. 4, pp. 232–235, Aug. 1997.

[3] D. Pearson, S. U. Pillai, and Y. Lee, "An algorithm for near-optimal placement of sensor elements," *IEEE Trans. Inform. Theory*, vol. 36, pp. 1280–1284, Nov. 1990.

[4] H. Alnajjar and D. W. Wilkes, "Adapting the geometry of a sensor subarray," in *Proc. Int. Conf. Acoust., Speech, Signal Process.*, vol. 4, Minneapolis, MN, 1993, pp. 113–116.

[5] X. Huang, J. P. Reilly, and M. Wong, "Optimal design of linear array of sensors," in *Proc. Int. Conf. Acoust., Speech, Signal Process.*, vol. 2, Toronto, ON, Canada, 1991, pp. 1405–1408.

[6] C. W. Ang, C. M. See, and A. C. Kot, "Optimization of array geometry for identifiable high resolution parameter estimation in sensor array signal processing," in *Proc. Int. Conf. Inform., Commun., Signal Process.*, vol. 3, Singapore, 1997, pp. 1613–1617.

[7] J.-W. Liang and A. J. Paulraj, "On optimizing base station antenna array topology for coverage extension in cellular radio networks," in *Proc. IEEE 45th Veh. Technol. Conf.*, vol. 2, Stanford, CA, 1995, pp. 866–870.

[8] Y. Hua, T. K. Sarkar, and D. D. Weiner, "An L-shaped array for estimating 2-D directions of wave arrival," *IEEE Trans. Antennas Propagat.*, vol. 39, pp. 143–146, Feb. 1991.

[9] M. Gavish and A. J. Weiss, "Array geometry for ambiguity resolution in direction finding," *IEEE Trans. Antennas Propagat.*, vol. 44, pp. 889–895, June 1996.

[10] N. Dowlut and A. Manikas, "A polynomial rooting approach to super-resolution array design," *IEEE Trans. Signal Processing*, vol. 48, pp. 1559–1569, June 2000.

[11] A. Manikas, A. Sleiman, and I. Dacos, "Manifold studies of nonlinear antenna array geometries," *IEEE Trans. Signal Processing*, vol. 49, pp. 497–506, Mar. 2001.

[12] V. H. MacDonald, "Optimum bearing estimation with passive sonar systems," Ph.D. dissertation, Yale Univ., 1971.
[13] M. Hawkes and A. Nehorai, "Effects of sensor placement on acoustic vector-sensor array performance," *IEEE J. Oceanic Eng.*, vol. 24, pp. 33–40, Jan. 1999.
[14] A. N. Mirkin and L. H. Sibul, "Cramér–Rao bounds on angle estimation with a two-dimensional array," *IEEE Trans. Signal Processing*, vol. 39, pp. 515–517, Feb. 1991.
[15] R. O. Nielsen, "Azimuth and elevation angle estimation with a three-dimensional array," *IEEE J. Oceanic Eng.*, vol. 19, pp. 84–86, Jan. 1994.
[16] M. A. Doron and E. Doron, "Wavefield modeling and array processing. III. Resolution capacity," *IEEE Trans. Signal Processing*, vol. 42, pp. 2571–2580, Oct. 1994.
[17] J. S. Bergin and K. L. Bell, "Wideband direction of arrival estimation for multiple aeroacoustic sources," in *Proc. Meet. MSS Specialty Group Battlefield Acoust., Seismics*, Laurel, MD, 2000.
[18] A. Nehorai and E. Paldi, "Vector sensor processing for electromagnetic source localization," in *Conf. Rec. Twenty-Fifth Asilomar Conf. Signals, Syst. Comput.*, vol. 1, New Haven, CT, 1991, pp. 566–572.
[19] A. Nehorai and M. Hawkes, "Performance bounds for estimating vector systems," *IEEE Trans. Signal Processing*, vol. 48, pp. 1737–1749, June 2000.

Ülkü Baysal (S'98) was born in Amasya, Turkey, in 1977. She received the B.S. degree from Middle East Technical University, Ankara, Turkey, in 1999 and the M.S. degree from The Ohio State University (OSU), Columbus, in 2002, both in electrical engineering. She is currently a Research Assistant at OSU, where she is pursuing the Ph.D. degree.

Her research interests include digital signal processing and sensor array processing.

Randolph L. Moses (S'78–M'85–SM'90) received the B.S., M.S., and Ph.D. degrees in electrical engineering from Virginia Polytechnic Institute and State University, Blacksburg, in 1979, 1980, and 1984, respectively.

During the summer of 1983, he was a SCEEE Summer Faculty Research Fellow at Rome Air Development Center, Rome, NY. From 1984 to 1985, he was with the Eindhoven University of Technology, Eindhoven, The Netherlands, as a NATO Postdoctoral Fellow. Since 1985, he has been with the Department of Electrical Engineering, The Ohio State University, Columbus, where he is currently a Professor. From 1994 to 1995, he was on sabbatical leave as a visiting researcher with the System and Control Group, Uppsala University, Uppsala, Sweden. His research interests are in digital signal processing and include parametric time series analysis, radar signal processing, sensor array processing, and sensor networks. He is coauthor, with P. Stoica, of *Introduction to Spectral Analysis* (Englewood Cliffs, NJ: Prentice-Hall, 1997).

Dr. Moses served on the Technical Committee on Statistical Signal and Array Processing of the IEEE Signal Processing Society from 1991 to 1994. He is a member of Eta Kappa Nu, Tau Beta Pi, Phi Kappa Phi, and Sigma Xi.